Sedimentary Geology xxx (2008) xxx–xxx

Contents lists available at ScienceDirect

Sedimentary Geology

journal homepage: www.elsevier.com/locate/sedgeo

Termination of the Arabian shelf sea: Stacked cyclic sedimentary patterns and timing (Oligocene/Miocene, Oman)

Markus Reuter [a,*], Werner E. Piller [a], Mathias Harzhauser [b], Andreas Kroh [b], Davide Bassi [c]

[a] *Institute for Earth Sciences, Geology and Palaeontology, Graz University, Heinrichstrasse 26, A-8010 Graz, Austria*
[b] *Natural History Museum Vienna, Burgring 7, A-1010 Vienna, Austria*
[c] *Dipartmento di Scienze della Terra, Università di Ferrara, via Saragat 1, I-44100 Ferrara, Italy*

ARTICLE INFO

Article history:
Received 19 June 2007
Received in revised form 26 August 2008
Accepted 2 September 2008
Available online xxxx

Keywords:
Facies
Peritidal carbonate cycles
Stratigraphy
Oligocene/Miocene transition
Arabian Shelf
Oman

ABSTRACT

In the Janabah region of southeastern Oman, Oligocene/Miocene limestones of the Shuwayr, Warak and Ghubbarrah formations are widely exposed. They were deposited on an extensive shallow carbonate platform that was part of the Arabian Shelf and located on the Gulf of Aden's northeastern rift shoulder, which emerged during the Early Miocene. The uppermost part of the studied sedimentary succession developed immediately before the permanently subaerial exposure of the carbonate platform. Cyclic changes of intertidal and subtidal facies document a fluctuating relative sea level at different frequencies and a continuous decline of accommodation. Single erosive surfaces with palaeokarst cavities and caliche crusts separate larger depositional cycles. These disconformities imply relatively long episodes of subaerial exposure and are interpreted to have been formed during lowstands of third-order sea level cycles that denuded the platform. Taxonomic studies of the accompanying mollusc faunas and certain benthic foraminifers allow a correlation of the recognised subaerial disconformities with the Ru4/Ch1 to Ch4/Aq1 sequence boundaries of Hardenbol et al. [Hardenbol, J., Thierry, J., Farley, M.B., Jacquin, T., Graciansky, P.-C., Vail, P.R., 1998. Mesozoic and Cenozoic Sequence Chronostratigraphic Framework of European Basins. In: Graciansky, C.-P., Hardenbol, J., Jacquin, T., Vail, P.R. (Eds.), Mesozoic and Cenozoic Sequence Stratigraphy of European Basins. Society for Sedimentary Geology, Special Publication 60, 13–603.]. This demonstrates that the termination of the Arabian shelf sea must be back-dated from the middle Burdigalian to the early Aquitanian.

1. Introduction

The collision of Africa and Eurasia during the Early Miocene and the resultant closure of the marine passage between the eastern and western Tethys (Tethyan Seaway) had far-reaching consequences for the distribution of shallow water areas and the course of ocean currents (Adams et al., 1983; Rögl, 1998). It was, therefore, one of the major events for the distribution and evolution of both terrestrial and marine faunas during the Cenozoic (Jones, 1999; Harzhauser et al., 2007). In this context, the termination of the Arabian shelf sea was an important step because of a drastic reduction of shallow water areas.

In this study, we elaborate a depositional model for the Oligocene/Miocene Shuwayr, Warak and Ghubbarrah formations in southeast Oman that were deposited on the Arabian Shelf and provide information about the plate motion as well as the sea level oscillations briefly before its final subaerial exposure. Due to the lack of age-diagnostic fossils in the shallow marine limestones, stratigraphic concepts were rough and based on lithostratigraphic correlation (Jones and Racey, 1994) and vague or erroneously determined assemblages of shallow water faunas (molluscs and benthic foraminifers; Platel et al., 1992b; Béchennec et al., 1993), which show a strong facies dependence and contain a high percentage of endemic elements (Harzhauser, 2007; Harzhauser et al., 2008). A further scope of this study is therefore to improve the existing litho- and biostratigraphic schemes by a sequence-stratigraphic model for the Shuwayr, Warak and Ghubbarrah formations that will help determine the timing of the Arabian Shelf emersion more precisely.

2. Geological setting and stratigraphy

Since the Paleocene, the Arabian Shelf was covered by an extensive shallow sea (Jones and Racey, 1994). It achieved its largest distribution during the Paleocene/Eocene Thermal Maximum, when it covered most of the Arabian Platform between eastern Somalia and eastern Saudi Arabia including southern Yemen, the Dhofar region, the interior of Oman, as well as the eastern margin of the already exposed Oman Mountains in northern Oman (Jones and Racey, 1994; Bernecker, 2006). The decline of the Arabian shelf sea was initiated by rifting in the Gulf of Aden and the southern Red Sea during the Oligocene and Early Miocene (Roger et al., 1989; Hughes et al., 1991;

* Corresponding author. Tel.: +43 316 380 8731; fax: +43 316 380 9871.
E-mail address: markus.reuter@uni-graz.at (M. Reuter).

0037-0738/$ – see front matter © 2008 Elsevier B.V. All rights reserved.
doi:10.1016/j.sedgeo.2008.09.001

Watchorn et al., 1998; Abbate et al., 2001; Huchon and Khanbari, 2003) that reduced the shelf to small isolated areas at the northern margin of the Oman Mountains and in southeast Oman already during the Oligocene (Jones and Racey, 1994; Bernecker, 2006). Thermal uplift of the rift flanks, which occurred with the onset of sea-floor spreading subsequent to the rifting stage, was responsible for the final emergence of the Arabian Shelf in the southern and western Arabia and is assumed to have begun during the middle Burdigalian (Camp and Robol, 1992; Daradich et al., 2003; Fournier et al., 2004).

The southern coast of Oman forms the northeastern passive margin of the Gulf of Aden. It comprises the Dhofar Plateau in the western part and the Jiddat-Arkad Plateau in the eastern part. Both regions are separated by the Jabal Qarabyan Fault which was not active during deposition of the studied Oligocene/Miocene sedimentary succession (Fournier et al., 2004). The Dhofar Plateau is mainly made up of Eocene carbonates, whereas in the Jiddard Arkard region Oligocene and Miocene carbonates prevail. In the southern direction the rift shoulder is bounded by the escarpments of Jabal Samhan, Jabal Qamar, and Jabal Qara from the Dhofar grabens (Fig. 1). The study area is located in the Janabah region, which is a part of the Jiddat-Arkad (Fig. 1). In this area, carbonates of the Dhofar Group and Fars Group form about 100-m-high coastal cliffs. In southeast Oman, the Dhofar Group includes the Shuwayr Formation, while in the Fars Group the Warak and Ghubbarrah formations are contained (Fournier et al., 2004).

The Oligocene/Miocene sedimentary succession was studied on Ras Madrakah (Fig. 1B). It starts with the Shuwayr Formation. This was defined southeast of Duqm in the cliffs south of the village Shuwayr (Fig. 1A) as white bioclastic reefal limestone with interbedded debris-flow deposits (interpreted differently in the present work), dolomitic laminated limestone and green reddish clay, as well as black dolomite at the top. Platel et al. (1992a,b) supposed a Late Oligocene to Early Miocene age for the Shuwayr Formation. The Shuwayr Formation forms the coastal cliffs between Duqm and Madrakah Peninsula. At Dill Beach on Madrakah Peninsula we logged the 116-m-thick Madrakah Cliff section (MC: N 19°01′31.36″, E 07°48′25.61″; Fig. 2A). At the base of the MC section, the Shuwayr Formation is in tectonic contact with the underlying Masirah ophiolite zone (Fournier et al., 2004). Beds dip with 30° to the southwest although, generally, the sub-horizontally lying beds dip to the northwest with 5–10°. In its lower part, the Shuwayr Formation comprises limestones that alternate with marl deposits, while in its middle segment pure limestones predominate. Upsection, the latter pass into a sequence of dolomitic limestones forming the top of the MC section, as well as a vast plain that covers large parts of Madrakah Peninsula.

Sediments of the Warak and Ghubbarrah formations were studied at a hill 5.6 km west of Dill Beach (Gebel Madrakah, section GM: N 19°02′19.11″, E 57°45′12.22″; Fig. 2B). The hill represents an erosional relic on top of the vast plain that is formed by the dolomitic cap of the Shuwayr Formation. The contact to the Shuwayr Formation, as well as the basal part (approximately 10 m) of the Warak Formation, is not exposed at the hill due to a cover of scree. Exposed is a 22-m-thick limestone succession, which is interpreted to be in sedimentary contact with the Shuwayr Formation according to consistent dip levels (5–10° northwest).

The Warak Formation was defined east of Shuwaymiyah in the catchment area of Wadi Warak by Platel et al. (1992a) as white to pink bioclastic limestone with interbedded coral-bearing debris-flow deposits, white chalky limestone, and reefal limestone. Platel et al. (1992a) assumed a Late Oligocene to Early Miocene age for the Warak Formation.

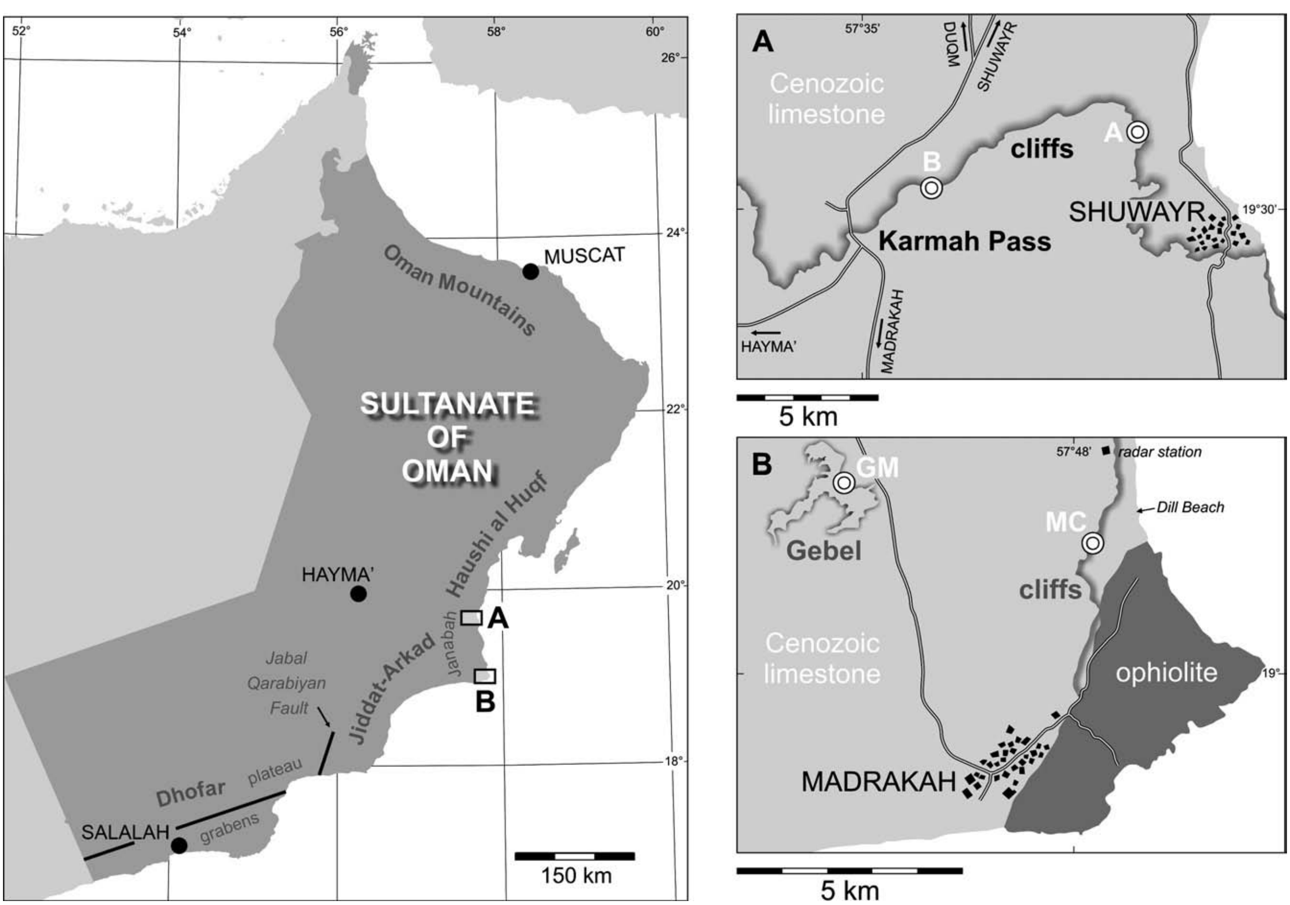

Fig. 1. Geographic maps of the Sultanate of Oman and of the studied locations in the Duqm District (A) and on the Madrakah Peninsula (B).

Please cite this article as: Reuter, M., et al., Termination of the Arabian shelf sea: Stacked cyclic sedimentary patterns and timing (Oligocene/Miocene, Oman), Sedimentary Geology (2008), doi:10.1016/j.sedgeo.2008.09.001

Fig. 2. Field aspects of Madrakah Peninsula. (A) Madrakah Cliffs at Dill Beach. The sub-horizontal beds of the Shuwayr Formation are laterally continuous over kilometres. Black hills at mid distance belong to the Masirah ophiolite zone. (B) Warak Formation and Ghubbarrah Formation (WF/GF) at Gebel Madrakah. The free-standing hill is an erosional relic on the vast plain formed by the dolomite cap of the Shuwayr Formation.

The shallow marine limestones of the overlying Ghubbarrah Formation also comprise a highly diverse fauna of large molluscs. Strombids and tridacnid bivalves are typical constituents of this fauna and missing in the Shuwayr and Warak formations (Béchennec et al., 1993; Harzhauser, 2007; Harzhauser et al., 2008). Because of the otherwise strong lithofacies similarities between the formations, we use the mollusc fauna (e.g., the occurrence of large strombids and of the bivalve genus *Tridacna*) as a criterion to distinguish the Ghubbarrah Formation from the Shuwayr and Warak formations. Platel et al. (1992b) assumed a Burdigalian to Langhian age for the Ghubbarrah Formation.

3. Facies

3.1. Shuwayr Formation (Fig. 3)

In its basal segment (beds 1–7), the MC section is characterised by marl lithologies (Fig. 3). It includes an 18-m-thick series of alternating grey marls, miliolid-grainstones, mudstones, and wackestones. Carbonate grains have micrite envelopes (cortoids). The associated fauna contains large lepidocyclinids with undulating tests (*Eulepidina fomosoides*) that are commonly enriched in coquinas (Fig. 4A), as well as a diversified non-constructional coral assemblage dominated by poritids and faviids with massive growth forms. Platy corals (cf. *Leptoseris*) are subordinate. Some lepidocyclinid coquinas contain abundant *Acropora* fragments. The corals and foraminifers are accompanied by molluscs (*Solariella krohi*, *Spondylus* sp., *Chlamys* sp.), decapods (*Callianassa* claws), echinoid spines (*Phyllacanthus* sp.), asteroids (Goniasteridae indet.), celleporiform bryozoans, as well as teeth of large sphyraenid fishes.

Above follows a 64-m-thick limestone unit representing the middle segment of section MC (beds 8–51). Grey, bioclastic packstones and grainstones with abundant miliolid foraminifers (amongst others *Archaias*, *Austrotrillina*, *Peneroplis*) and peloids dominate. Carbonate grains have micrite envelopes (cortoids). In some beds, coralline red algae and small lenticular lepidocyclinids (*Nephrolepidina* cf. *morgani*) contribute essentially to the sediments. Scattered colonial corals with large (up to 70 cm length) massive colonies in growth position are surrounded by skeletal debris, and small patch reefs are present in this facies. The latter are constructed either by foliaceous corals (cf. *Leptoseris*) or dominated by branching corals. Massive corals contribute only minimally to the framework. Bed 23 contains *Acropora* fragments. Gastropods (see Harzhauser, 2007), bivalves (e.g., "*Pinna*", *Kuphus* sp.), echinoids (e.g., bed 19: cidaroids, burrowing spatangoids; bed 29: *Clypeaster* sp., *Tripneustes* sp.) and asteroids (Goniasteridae indet.) are further abundant faunal constituents. Fenestrate bryozoans (beds 19, 47) and octocorallia internodes additionally occur in some beds.

Intercalated are limestone and dolomite beds with a wavy lamination on mm- and cm-scale. Cross-bedded miliolid-grainstone with flat pebbles of dolomite occurs as well. Straight, 10 cm deep cracks are locally associated with the miliolid-grainstone facies and form ramose networks with orthogonal intersections on the top surfaces of beds 13 and 42 (prism cracks). Rootlets are common in some beds and preserved as tubular voids or concretions (<1 cm in diameter). Typically, these voids/concretions are fringed by fine-grained cement and exhibit downward bifurcations with decreasing diameters of lower order branches forming ramified networks (Fig. 5A, B). This distinguishes them from bioturbations produced by burrowing organisms (Klappa, 1980). Other limestone beds contain potamidid coquinas with *Pyrazisinus monstrosus* and *Granulolabium* sp. that are associated with rootlets or an erosive surface at the top of bed 9.

Two distinct erosive surfaces are present in this unit: one at the top of bed 9, another at the top of bed 28. The first has an irregular relief with peaks and pockets (<10 cm difference in level), which indicates karstification (Fig. 6A). Depressions are filled with red mottled packstone (bed 10). Its red colour points to reworking of residual sediment. The second erosive surface exhibits voids of unregular size and shape that reach 0.4 m deep into bed 28 (Fig. 6B). They are filled with a poorly-sorted and component-supported breccia (Fig. 6C). The components consist of angular and subrounded, light grey limestone clasts (subtidal facies). The interstitial space is filled with red mudstone. According to Jones (1992), who recorded similar void-filling deposits from karstified Tertiary limestones on the Cayman Islands (Caribbean Sea), we interpret the voids as palaeokarst cavities

Please cite this article as: Reuter, M., et al., Termination of the Arabian shelf sea: Stacked cyclic sedimentary patterns and timing (Oligocene/Miocene, Oman), Sedimentary Geology (2008), doi:10.1016/j.sedgeo.2008.09.001

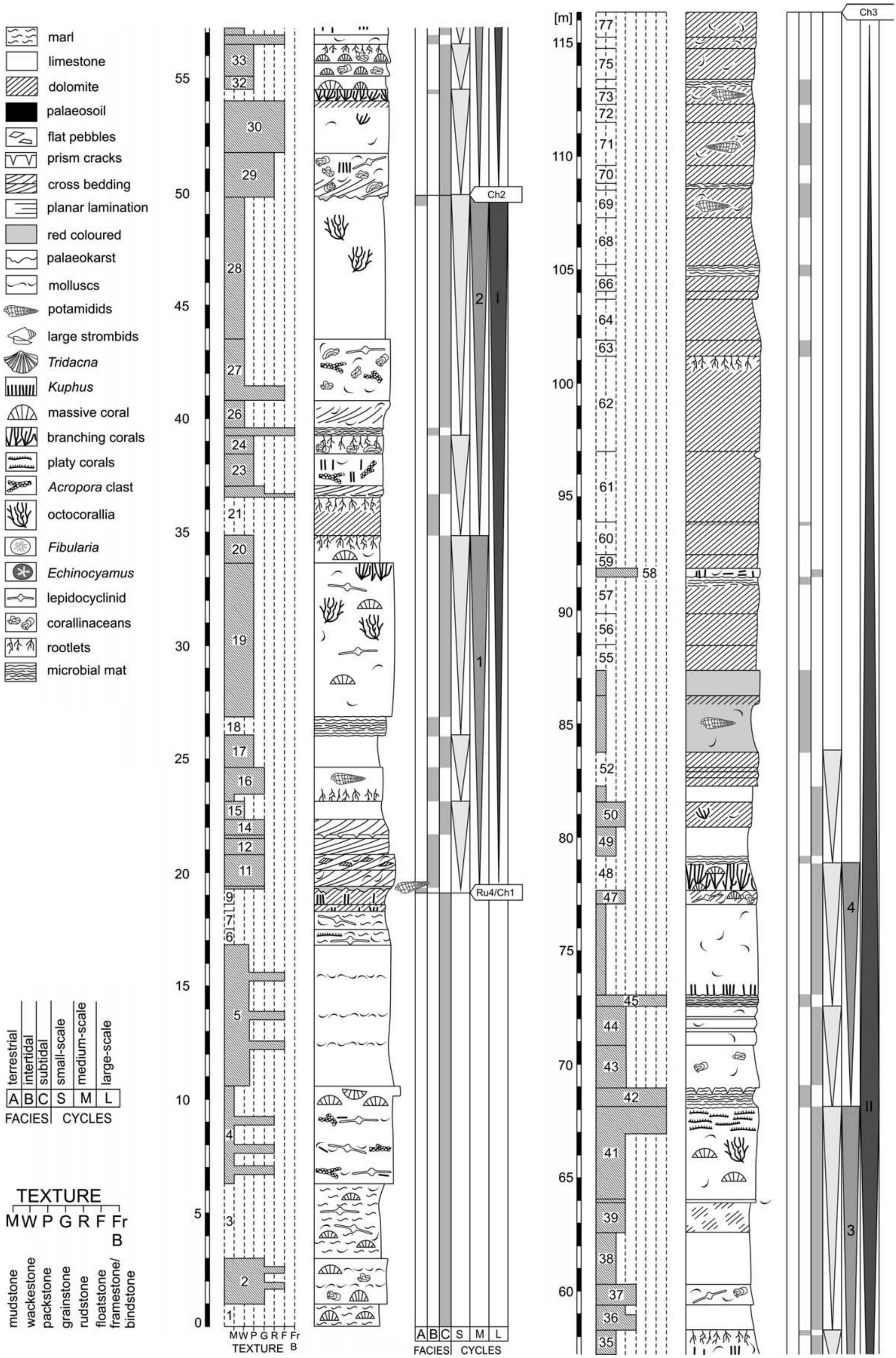

Fig. 3. Madrakah Cliff section (MC). Lithological log, facies, depositional cycles, and third-order sequence boundaries of the Shuwayr Formation.

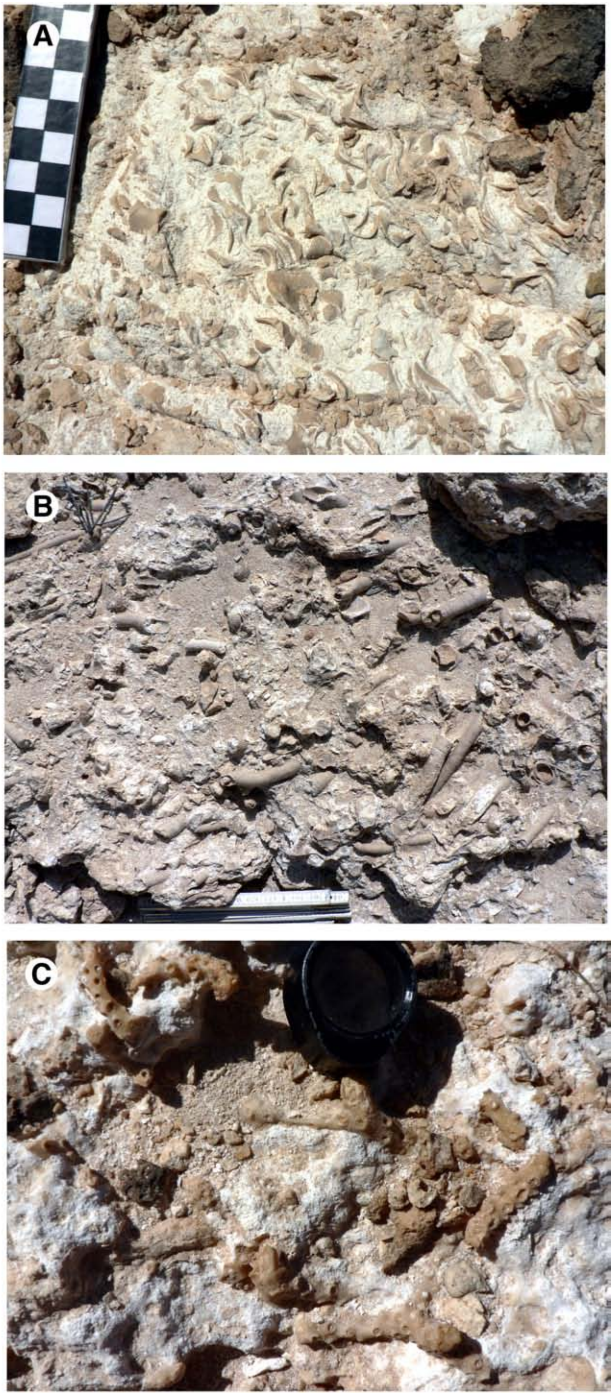

Fig. 4. Shallow marine biotic assemblages. (A) *Eulepidina formosoides* coquina in the lower part of the Shuwayr Formation at the Madrakah Cliff section. The large undulating tests of the foraminifers point to a shallow turbid environment; MC4, square length on the scale bar is 1 cm. (B) *Kuphus* pavement in the Warak Formation with toppled and *in situ* tubes. *Kuphus* accumulations preferentially occur in the immediate subtidal zone; Karmah Pass 3. (C) *Acropora* rubble in the Warak Formation; hand lens for scale, GM3.

and the encased sediment as collapse breccia, intermixed with redeposited palaeosoil sediment (terra rossa breccia *sensu* Jones, 1992).

The upper 34 m of section MC (beds 52–71) are dominated by dolomite. Dolomitization has destroyed most of the primary sedimentary textures as well as fossils, and the dolomite has a vuggy texture. At the base of the dolomite succession, red mudstones with potamidids are intercalated. Some dolomite beds contain layers of rich potamidid gastropod casts, casts of rootlets, or *in situ* and broken *Kuphus* tubes. Others show a wavy lamination on mm- and cm-scale or exhibit a red colour. Laminites and potamidid coquinas become more frequent towards the top of the section. A typical ichnoassemblage with *Thalassinoides* and *Gyrolites* occurs in this segment of the section.

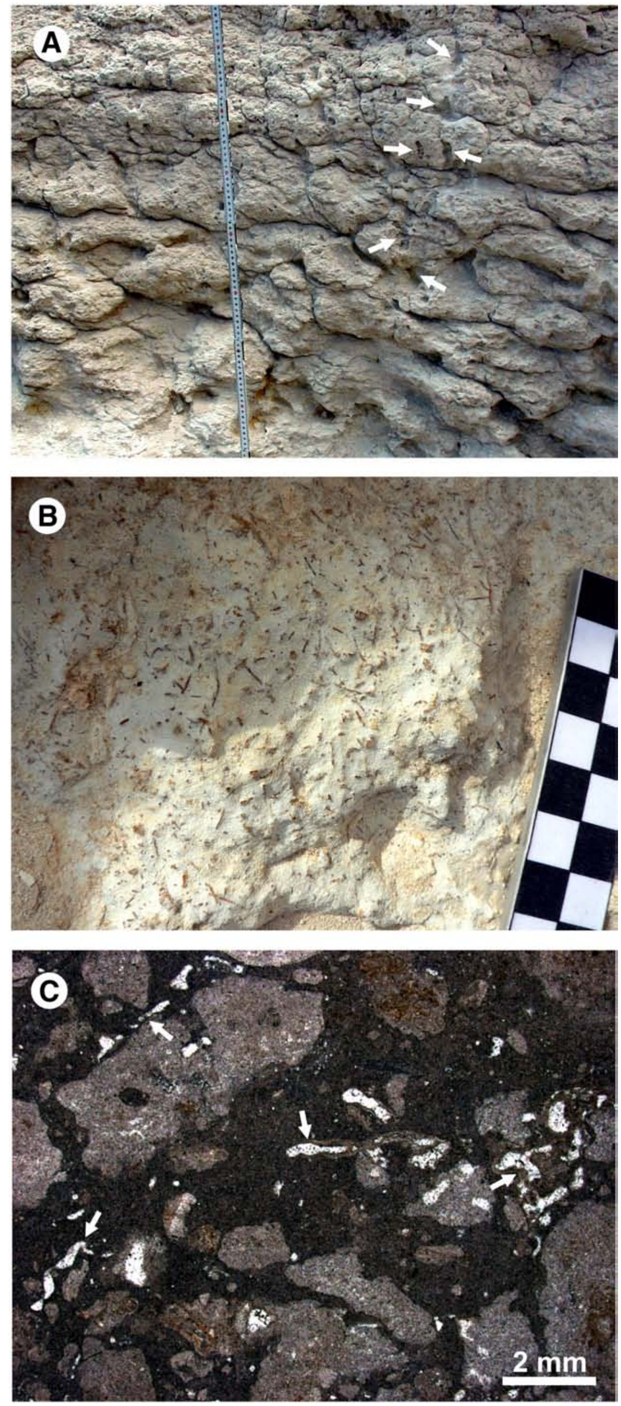

Fig. 5. Rootlets as indicators for intertidal and terrestrial environments. The presence of higher plants in intertidal and terrestrial environments is documented by tubular voids or concretions. In contrast to animal burrows they exhibit downward bifurcations with decreasing diameters of lower order branches. (A) Voids of well-developed taproots (arrows indicate the extent of main roots). The associated potamidid fauna document the presence of mangroves. Flaser bedding points to intertidal environment; MC16. (B) Small secondary roots forming a dense meshwork between the taproots. The rootlets are filled with brownish dolomite; square length on the scale bar is 1 cm, MC16. (C) Microphotograph of caliche crust with irregularly bent and branching voids, infilled with fine sparite (arrows). Such pedotubules refer to tiny rootlets of higher plants (Flügel, 2004); Karmah Pass 5.

3.2. Warak Formation (Fig. 7)

The exposed part of the Warak Formation (GM: beds 1–20) includes a 17-m-thick limestone succession (Fig. 7). Grey, bioclastic

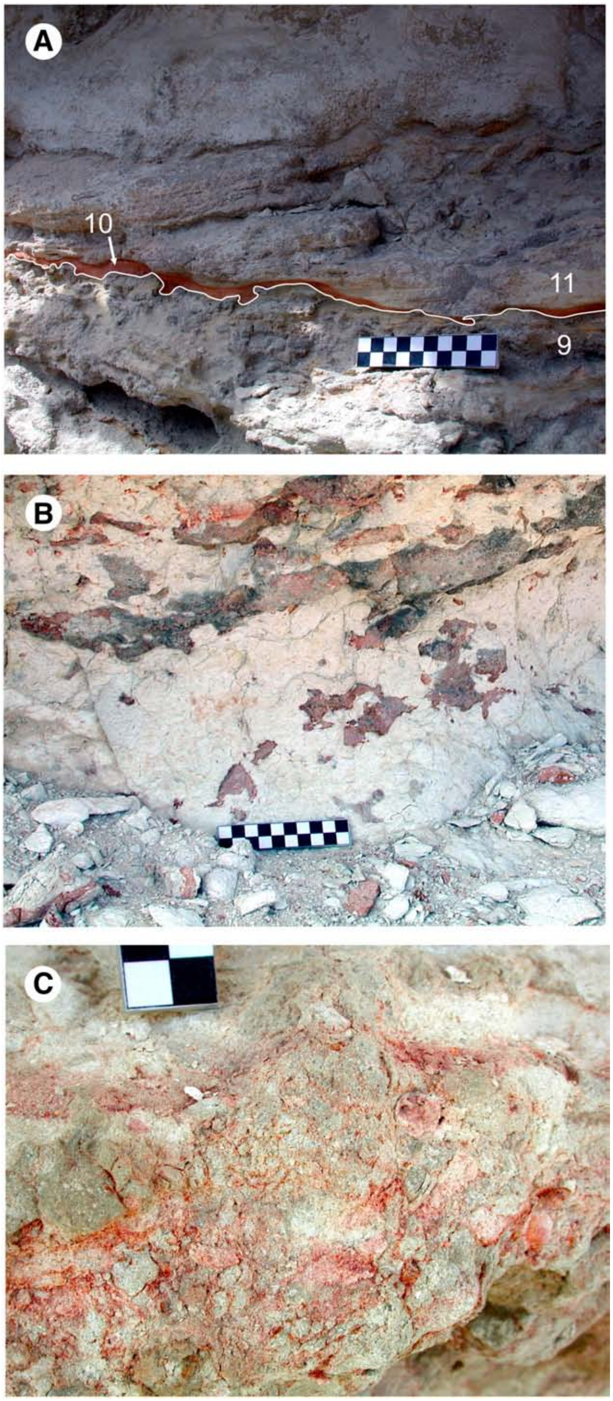

Fig. 6. Palaeokarst. (A) Erosive surface (white line) at the base of large-scale depositional cycle LI. It exhibits a distinct relief with peaks and pockets, which point to karstification in terrestrial environment. Depressions are sealed with potamidid-bearing packstone (10: highlighted in red). The red mottled colour of the sediment indicates reworking of residual sediment in the intertidal zone. Cross-bedded grainstone follows above (11) and indicates shallow subtidal conditions; numbers refer to beds in section MC (Fig. 3), the scale bar is 10 cm. (B) Cavities at the top of large-scale depositional cycle LI; bed MC28, the scale bar is 10 cm. (C) The void-filling deposit is a poorly-sorted, component-supported beccia, composed of light grey limestone clasts interpreted as collapse breccia. The remaining interstitial space of the breccia is filled with red mudstone, interpreted as incorporated palaeosoil; square length on the scale bar is 1 cm.

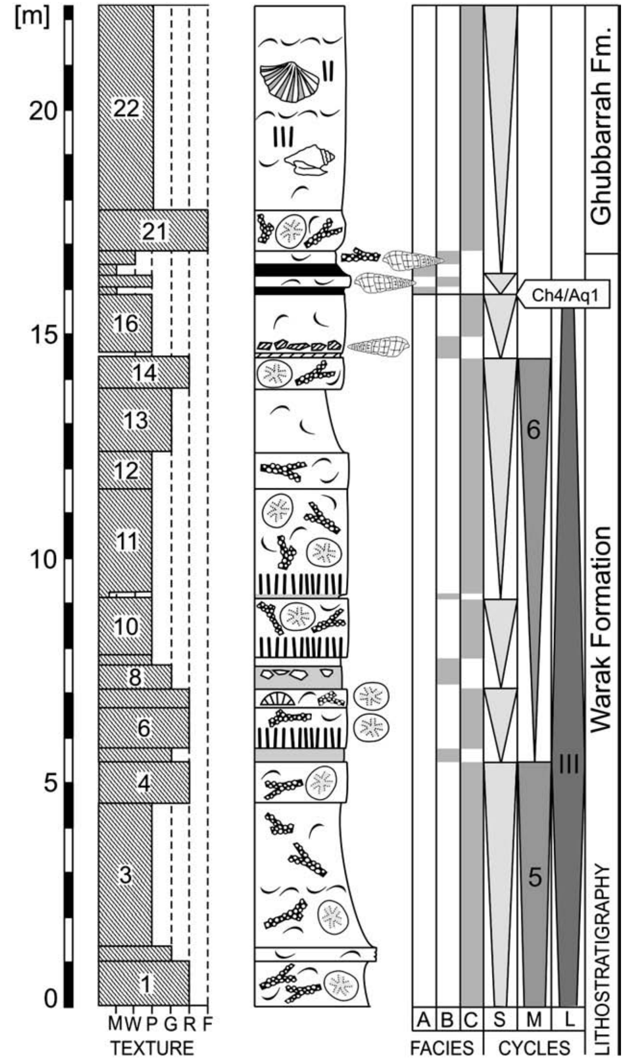

Fig. 7. Gebel Madrakah section (GM). Lithological log, facies, depositional cycles and third-order sequence boundaries of the Warak and Ghubbarrah formations. For key of signatures see Fig. 3.

miliolid-peloid packstones, rudstones and grainstones prevail. Carbonate grains have micite envelopes. The fauna is dominated by foraminifers. Miliolids (amongst others *Archaias*, *Austrotrillina*, *Peneroplis*) are dominant, textulariids and alveolids (*Borelis*) are common. The tiny clypeasteroid echinoid *Fibularia dubarensis* occurs in masses. Corals are frequent and mainly represented by masses of broken arborescent *Acropora* (Fig. 4C) and large (<50 cm height) massive *in situ* corals, as well as solitary corals. In some beds, small (<5 cm diameter) globular coral colonies with a central tube-like cavity occur (beds 4, 6, 7, 10, 11, 14). In beds 1 and 4 they are associated with nodular colonies of celleporiform bryozoans, also with a tube-like cavity in the centre. Molluscs are also abundant and highly diverse (see Harzhauser, 2007; and Harzhauser et al., 2008 for details). Typical features are *Omanidacna eos* coquinas (bed 3), and mass occurrences of *Strombus bernielandaui*. Cerithiids (*Cerithium rude*, *Cerithium markusreuteri*, *Cerithium archiaci*, *Gourmya baluchistanensis*, *Rhinoclavis submelanoides*), archaeogastropods (*Canthaidus elkeae*, *Tectus loryi*), *Warakia pilleri*, *Capulus anceps*, *Conorbis protensus*, and *Terebra perturrita* are common as well. These shells are usually well preserved and occur in large numbers. Others, such as *Campanile gigas* and *Pyrazisinus monstrosus* are less abundant and display strongly corroded shells. Single *Kuphus* tubes or *Kuphus* patches are distributed over a whole bed of bioclastic limestone, while layers with dense *in situ* tubes developed preferentially at the base of such a bed (Fig. 4B).

Please cite this article as: Reuter, M., et al., Termination of the Arabian shelf sea: Stacked cyclic sedimentary patterns and timing (Oligocene/Miocene, Oman), Sedimentary Geology (2008), doi:10.1016/j.sedgeo.2008.09.001

Intercalated in the grey, bioclastic limestones are red-stained limestone beds (beds 5, 8, base of bed 11) and a thin dolomite horizon (bed 15). The latter is covered by a layer of flat dolomite clasts and potamidid shells. The top of the Warak Formation is formed by two beds of green micrite that exhibit an inhomogeneous, breccia-like packstone texture with nodular fabrics (Fig. 5C). Spar filled micro-cracks occur circumgranular around micrite nodules or dissected the sediment as straight or wrinkled cracks. Fossils are absent but calcified tubules <1 mm are commonly present in this facies (Fig. 5C). All these features are mentioned by Flügel (2004) for caliche. The caliche beds alternate with gastropod-packstones with abundant potamidids.

3.3. Ghubbarrah Formation (Fig. 7)

The Ghubbarrah Formation following above (section GM: beds 21–22) is an erosional relic with only 4 m thickness. It is capped by an erosive surface with karst cavities filled up with red terrigenous material. Preserved are bioclastic packstones to floatstones with peloids, foraminifers (frequent miliolids, rare textulariids), and mollusc and echinoderm debris. Carbonate grains have micrite envelopes. The Ghubbarrah Formation yields a highly diverse mollusc fauna that differs from that of the Warak Formation in its composition and is described in detail by Harzhauser (2007). Typical constituents are gastropods (e.g. *Campanile pseudoobeliscus*, *Cantharidus elkeae*, *Cerithium rude*, *Gourmya delbosi*, *Mitra* cf. *dufresni*, *Pachycrommium harrisi*, *Warakia pilleri*). Large strombids (*Strombus gijskronenbergi*, *Dilatilabrum sublatissimus*) are often accumulated in coquinas. *Tridacna* bivalves and patchy *in situ* populations of the teredinid bivalve *Kuphus* are as well typical. Moreover, the preservation of fossils as silicified casts is a feature that distinguishes the Ghubbarrah Formation from the underlying Warak Formation, which displays exclusively calcite pseudomorphs.

4. Sedimentary environments

Abundant *in situ* corals in the lower marly part of the Shuwayr Formation (Fig. 3) as well as intercalated miliolid-grainstones and the absence of plankton document a shallow marine environment. However, the large size and undulating shape of lepidocyclinids (Fig. 4A), together with the dominance of associated massive poritid and favid corals, as well as platy cf. *Leptoseris* colonies, point to turbid conditions with low-light penetration (Wilson and Lokier, 2002).

The middle and upper part of the Shuwayr Formation (Fig. 3), as well as the Warak and Ghubbarrah formations (Fig. 7), formed in terrestrial, intertidal, and shallow subtidal environments (Fig. 8). The terrestrial facies is characterised by palaeokarst (Fig. 6) and caliche crusts (Figs. 5C, 8A, B).

Prism cracks in pure grainstone lithologies in association with flat dolomite pebbles reflect temporary desiccation in the intertidal zone and a hypersaline milieu where dolomite was formed (Cowan and James, 1992; Pratt et al., 1992). This environment favoured the development of microbial mats that produced the wavy bedded laminites (Fig. 8C). These microbial laminites could be associated with rootlets (Fig. 8C, D). At protected, tropical coasts the tidal zone is mostly occupied by mangroves which extend down to the low tide mark within the lower part of the tidal zone (Kathiresan and Bingham, 2001; Davis and Fitzgerald, 2004). Flaser bedding (Fig. 5A) and potamidid coquinas in rooted horizons refer to intertidal flats, which were colonized by mangroves (e.g., modern relatives of the potamidids *Terebralia* and *Pyrazisinus* are typical mangrove dwellers; Vohra, 1965; Houbrick, 1991). Red mudstones document intertidal flats as well (Haas et al., 2007).

The subtidal zone is characterised by carbonate sand deposits (Fig. 8E, F, H, J). Miliolid foraminifers and peloids contribute mainly to the carbonate sand (Fig. 8F). The high abundance of miliolids and peloids, as well as cortoids, indicate a shallow, lagoonal environment. The subtidal facies commonly starts with dense *in situ Kuphus* populations (Fig. 4B) or with well-sorted, cross-bedded miliolid-grainstones (Fig. 8E, F). The latter accumulated as sand waves in the shallowest parts of the subtidal zone. In slightly deeper environments, non-framework forming coral communities occurred (Fig. 8G, I). The mass occurrence of porcellaneous foraminifers, including abundant *Archaias* and *Peneroplis* (Fig. 8H), point to seagrass meadows (Sen Gupta, 1999). Seagrass vegetation is also indicated by bioimmuration in small globular corals and bryozoan colonies (Fig. 8G) (Cigliano et al., 2006), specialized echinoids (*Tripneustes* sp.; Lawrence and Agatsuma, 2001), and by *in situ* occurrences of “*Pinna*” (Hofrichter, 2002). Fenestrate bryozoans also populate commonly the shaded environments on seagrass rhizomes (Hofrichter, 2002). Intercalated mass accumulations of arborescent *Acorpora* fragments (Fig. 4C) document the intermittent presence of extensive *Acropora* carpets. Their modern counterparts favour a shallow water depth down to 7 m (e.g., Lighty et al., 1982; Piller and Riegl, 2003; Soong and Chen, 2003; Vargas-Ángel et al., 2003). Coarse-grained skeletal limestones with high contents of corallinaceans, associated lepidocyclinids (Fig. 8J) and octocorallia, as well as small patch reefs demonstrate more open-marine conditions (Gischler and Hudson, 1998). However, the high abundance of corals, the small lenticulid shapes of larger foraminiferan tests (Renema and Troelstra, 2001) (Fig. 8J), and the absence of plankton point to a persisting shallow water depth. Nevertheless, sporadically occurring octocorallia indicate a water depth that probably exceeded 10 m (Hughes Clarke and Keij, 1973).

5. Relief and hinterland

55 km northeast of the Madrakah Peninsula, further outcrops in shallow marine carbonates of the Dhofar and Fars groups exist in the Duqm District (Fig. 1A). For the comparison of sedimentary facies with the Madrakah sections, a representative 50-m-thick section of the Shuwayr Formation in the Duqm District (Fig. 9A) was logged along coastal cliffs north of the village of Shuwayr, near the type locality of the Shuwayr Formation (section Shuwayr Cliff, N 19°32′38.95″, E 57°41′00.63″). The Shuwayr Cliff section includes the upper segment of the Shuwayr Formation. The very top of the Shuwayr Formation is not exposed in this section, but in the nearby type section it consists of several metres of dolomite (Platel et al., 1992b; own observation). The Warak and Ghubbarrah formations were studied in a 17-m-thick section at Karmah Pass south of the pass road (section Karmah Pass, N 19°30′37.36″, E 57°35′22.56″) (Fig. 9B). Unfortunately, neither the contact to the underlying nor to the overlying lithostratigraphic unit is exposed at these localities. In combination with the lack of biostratigraphically relevant fossils, this makes a high-resolution stratigraphic correlation with the Madrakah sections difficult.

Despite their far distance, a comparative facies analysis of both study areas shows a very similar lithological succession and sedimentary environments in both the Madrakah and Duqm District, comprising intertidal facies with dolomite and microbial laminites and subtidal seagrass meadow and *Acropora* carpet facies (Harzhauser, 2007). The extensive and laterally consistent lithologies point to a subdued sea-floor topography of a very shallow and episodically emergent platform in the Jiddat-Arkad region (Fig. 10). Contradicting palaeoenvironmental reconstructions (as deeper fore-reef facies in a slope setting) possibly resulted from the misinterpretation of *Acropora* accumulations (Fig. 4C) as allochthonous reef debris (Platel et al., 1992b; Béchennec et al., 1993). In our opinion, however, the platform was covered with extensive *Acropora* carpets during some periods. The fragile coral carpets were regularly destroyed in the shallow environment (Gischler, 2008) and the *Acropora* rubble was deposited more or less on site.

Despite repeated subaerial exposure and erosive events, no continentally derived lithic grains occur in any of the studied sections, neither at Madrakah Peninsula nor in the Duqm District. This is

Please cite this article as: Reuter, M., et al., Termination of the Arabian shelf sea: Stacked cyclic sedimentary patterns and timing (Oligocene/Miocene, Oman), Sedimentary Geology (2008), doi:10.1016/j.sedgeo.2008.09.001

evidence for a far distant hinterland and a tectonically stable platform. Potential source areas for terrigenous material were the Oman Mountains and the Haushi-Huqf Uplift that formed islands in the east (Béchennec et al., 1993), or the larger landmass of the Western Arabian Highlands in the northwest (Jones and Racey, 1994) (Fig. 10). At the Oligocene/Miocene transition, the crystalline Precambrian core of the Haushi-Huqf Uplift possibly was covered by Cretaceous and Paleogene limestones (Filbrandt et al., 1990) and no source for

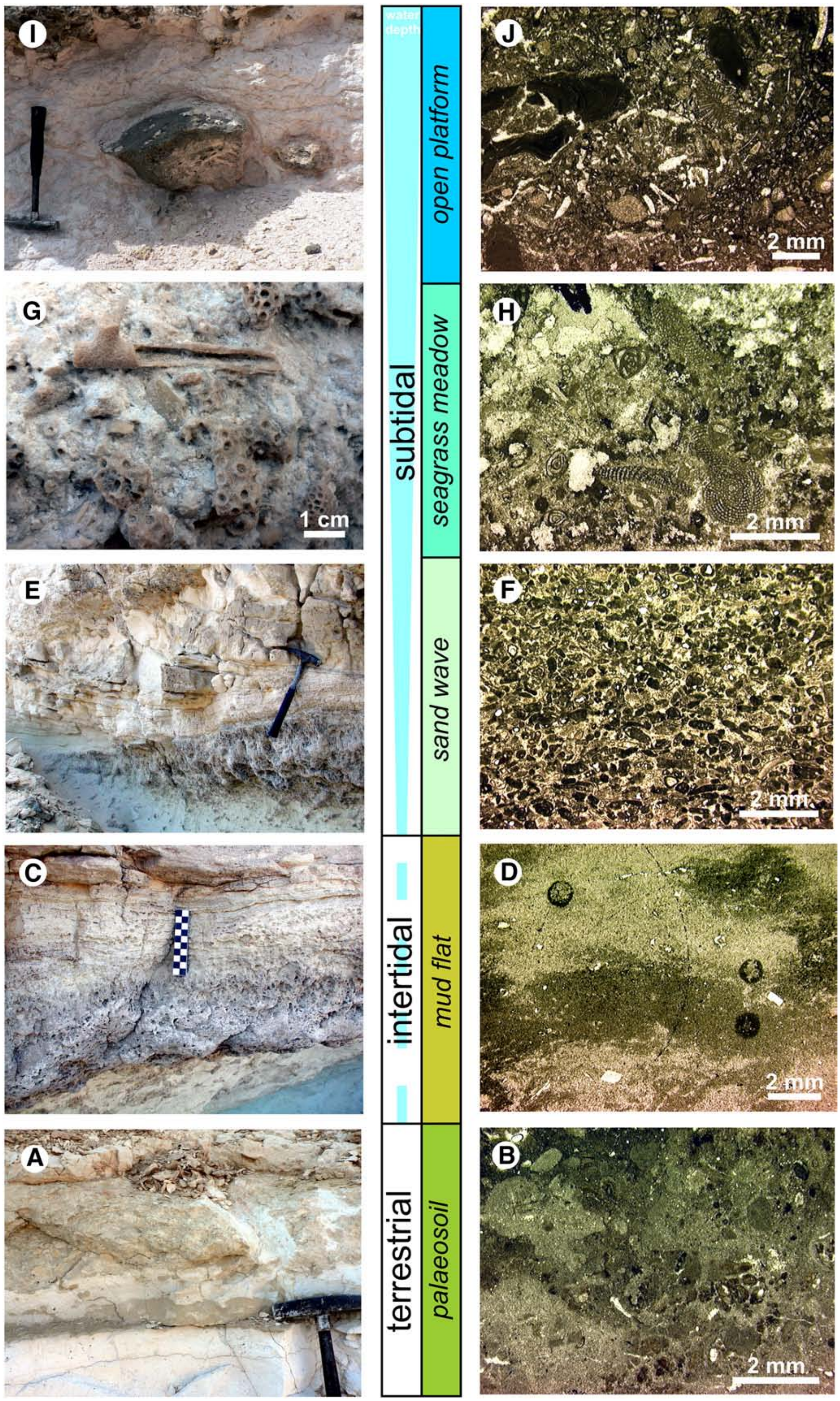

siliciclastics. Coarse terrigenous material that derived from the exposed Oman Mountains was caught in the Suneinah Trough (Béchennec et al., 1993), and the Arabian Highlands were situated too far away to have allowed input of coarse-grained terrigenous material onto the Jiddat-Akard Platform (Fig. 10). Even clay minerals reached the interior platform as suspension load only during deposition of the lower part of the Shuwayr Formation (Fig. 3). Possibly, the argillaceous sediments at the base of section MC reflect a more humid climate, when continental runoff washed huge amounts of clay into the sea. Instead, the upper part of the Shuwayr Formation reflects a more arid climate that caused sediment starvation and intermittent evaporation of the interior platform. To the southwest the platform opened to the graben systems of the Dhofar region (Fournier et al., 2004) (Fig. 10), where the Mughsayl Formation was deposited in deeper open-marine environments (Jones and Racey, 1994).

6. Cyclic sedimentary patterns

A striking feature of the middle and upper Shuwayr Formation, the Warak Formation, and the Ghubbarrah Formation is a cyclic stacking of supratidal, intertidal and subtidal facies (Figs. 3, 7, 9) that is missing in older shallow marine Cenozoic shelf deposits from Oman (Beavington-Penny et al., 2006). In our study, three hierarchies of cycles could be distinguished that document a fluctuating relative sea level at different frequencies.

6.1. Small-scale cycles

Small-scale depositional cycles comprise a gradual facies change from intertidal facies to subtidal facies that document deepening of the environment. Most small-scale cycles have a thickness of 2 m to 5 m. Their 1–4 m thick subtidal parts are characterised by restricted, shallow subtidal facies. Typical for these relative thin subtidal units are dense *Kuphus* populations (Fig. 4B) and a *Thalassinoides–Gyrolites* ichnoassemblage. Less common are 5–10 m thick subtidal units, which comprise more open-marine facies.

6.2. Medium-scale cycles

Medium-scale depositional cycles are in the order of 10 m to 20 m thick. They start with a bundle of two or three small-scale cycles that indicate a low-amplitude but high-frequency fluctuating relative sea level. The uppermost small-scale cycle of a medium-scale cycle is characterised by a thick subtidal member (5–10 m). This indicates opening of the platform and installation of a stable, deeper subtidal environment that contains in some cases also more open-marine facies. The upward-increasing thickness of the small-scale cycles suggests increasing accommodation space from the bottom to the top of a medium-scale cycle.

6.3. Large-scale cycles

Large-scale depositional cycles have a thickness of some tens of metres and are separated by major unconformities in the sedimentary record. At Ras Madrakah, the Shuwayr Formation comprises two distinct erosive surfaces, at the top of bed MC9 and at the top of bed MC28. These reflect exposure of the shallow platform due to long-lasting lowstands of relative sea level. Another subaerial episode during a low relative sea level is reflected in the Madrakah area by caliche deposits at the top of the Warak Formation (Figs. 5C, 7, 8A, B). A prominent caliche bed intercalated in the Karmah Pass section (Fig. 9B) possibly corresponds to this lowstand.

A prominent fall of relative sea level is reflected in the dolomite cap of the Shuwayr Formation (Fig. 3). The dolomitization, however, did not affect sediments of the Warak and Ghubbarrah formations (Fig. 7), which conformably overlay the Shuwayr Formation. The formation of this dolomite is therefore considered to be an early diagenetic process that occurred before deposition of the Warak and Ghubbarrah formations during an episode with long-term restriction. Because the thick dolomite cap at MC is composed of distinct beds (Fig. 3) it is well possible that these beds reflect high-frequency sea level fluctuations. However, facies changes are not discernible because of strong dolomitization. This indicates dolomitization was a multiphase process and every small-scale cycle underwent penecontemporaneous dolomitization before the following cycle was deposited. This may correspond to a late highstand situation.

From the recognition of major emersion and restriction events on the interior platform, three large-scale cycles (LI, LII, LIII) can be distinguished in the studied section: two large-scale cycles that form the middle and upper segment of the Shuwayr Formation (LI, LII) (Fig. 3) and one large-scale cycle that represents the Warak Formation (LIII) (Fig. 7). Each large-scale depositional cycle starts with thick medium-scale cycles with thick subtidal parts at their top (Figs. 3, 7). The important thickness of medium-scale cycles and deep subtidal facies indicate a general increase in accommodation during large-scale maximum flooding (Goldhammer et al., 1990; Strasser et al., 1999). Above follows a karstified surface (Fig. 3: top of LI) that indicates a rapid fall of relative sea level and a long emersion period (Strasser, 1991). Alternatively, the thick medium-scale cycles are covered by a succession of thin medium-scale depositional cycles which end with thin subtidal members (Fig. 3: LII, Fig. 7: LIII). The latter may pass into a succession of small-scale depositional cycles (Fig. 3: top of LII) or are covered by caliche (Figs. 7, 9: top of LIII). These thinning and shallowing upward trends point to a general decline in accommodation during a large-scale late highstand (Strasser et al., 1999).

7. Timing of the Arabian Shelf emersion

A prerequisite for the stacking of peritidal carbonate cycles is the creation of accommodation space by subsidence and/or long-term eustatic sea level rise (Drummond and Wilkinson, 1993; Demicco, 1998). Furthermore, especially in shallow peritidal settings also minor, low-amplitude sea level changes are commonly recorded (Strasser et al., 1999; Schlager, 2005; Paterson et al., 2006). Therefore, we expect the analysis of cyclicity patterns to provide information about the plate motion as well as the sea level oscillations briefly before the final subaerial exposure of the Arabian Shelf. Strasser et al. (1999) show that based on one section alone it is tricky to correctly interpret the observed stacking pattern, even if the general time framework is

Fig. 8. Field aspects and microfacies of sedimentary environments as an estimate for the relative palaeo-water depth in a complete depositional cycle. (A) Caliche crust that formed during subaerial exposure; GM17, hammer for scale. (B) Thin section of caliche crust with inhomogeneous, breccia-like packstone texture, nodular fabrics, and spar-filled microcracks; Karmah Pass 5. (C) Laminated microbial mat. The early diagenetic formation of dolomite in the intertidal environment destroyed the lamination at the base of the bed; MC18, the scale bar is 10 cm. (D) Dolomite with rhomboidal dolomite crystals and cross sections of rhizocretions on an intertidal mudflat. The dark fine crystalline rims developed by preferential cementation of the sediment surrounding a decaying root; base of bed MC18. (E) Cross-bedded grainstone covering a microbial mat. This facies represents sand waves that formed in a shallow subtidal environment; MC22, hammer for scale. (F) Miliolid-grainstone. The mass occurrence of porcellaneous miliolids reflects a shallow, lagoonal environment. The excellent winnowing and sorting points to turbulent water; MC22. (G) Coral-bryozoan limestone. Small nodular coral colonies and elongated bryolites are pierced by tube-like cavities that possibly resulted from decayed seagrass on which the organisms grew; GM4. (H) Foraminiferal grainstone. The foraminifers are dominated by miliolids (among others *Archaias* and *Austrotrillina*), indicating a seagrass environment; MC36. (I) Non-framework forming massive coral colonies (*in situ*); Shuwayr Formation, Ras Madrakah, hammer for scale. (J) Packstone with corallinaceans and *Nephrolepidina* cf. *morgani* documenting more open-marine conditions; MC47.

Please cite this article as: Reuter, M., et al., Termination of the Arabian shelf sea: Stacked cyclic sedimentary patterns and timing (Oligocene/Miocene, Oman), Sedimentary Geology (2008), doi:10.1016/j.sedgeo.2008.09.001

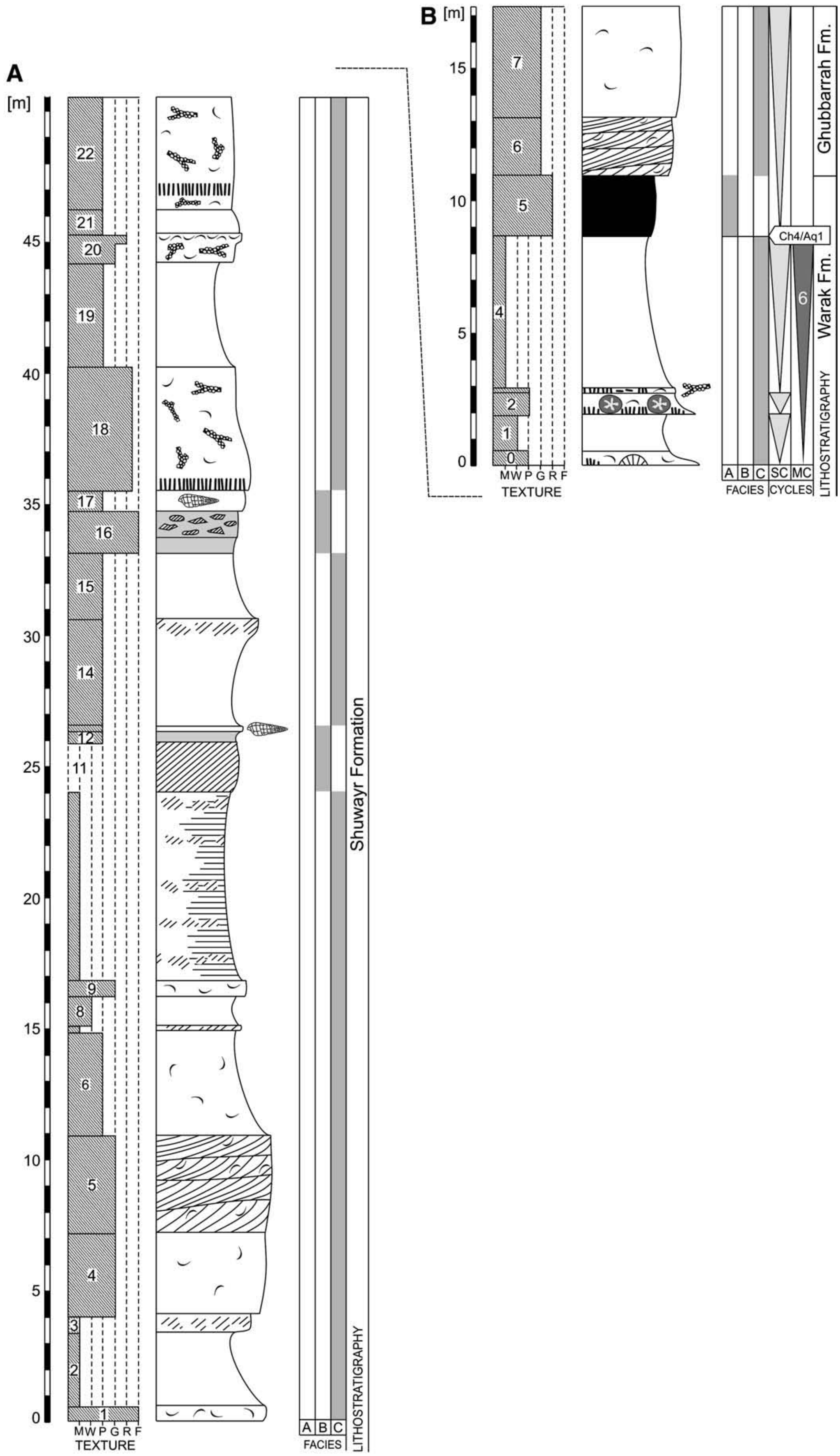

Fig. 9. Measured sections of the Shuwayr Formation (Shuwayr Cliff section: A), Warak and Ghubbarrah formations (Karmah Pass section: B) in the Duqm District. Lithologic log, facies, depositional cycles and third-order sequence boundaries. For key of signatures see Fig. 3.

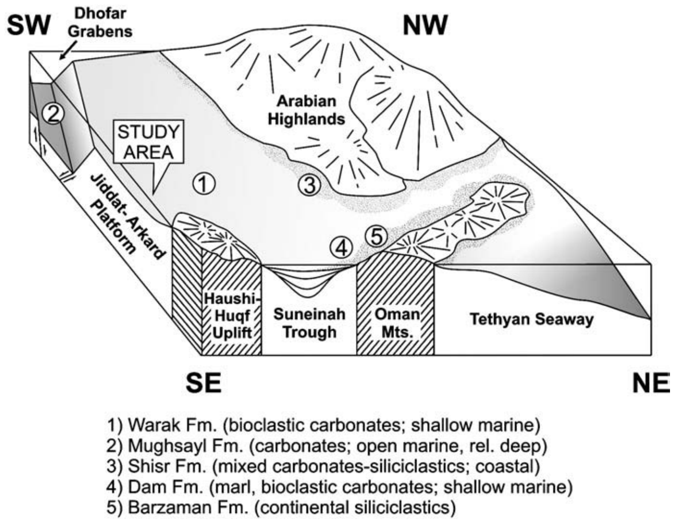

Fig. 10. Schematic sketch illustrating the Late Oligocene palaeogeography of the Arabian Shelf in the area of Oman. Compilation after Béchennec et al. (1993), Jones and Racey (1994), and Fournier et al. (2004).

given. They suggest that long-distance correlations of sections are necessary to filter out autocyclically formed depositional sequences and identify local and regional gaps in the sedimentary record. Nonetheless, widespread erosion (base of LI, LII, top of LIII) and intertidal overprinting of subtidal facies (top of LII) point to a drop of sea level that produced well-defined sequence boundaries (Bosselini, 1989; Strasser, 1991; Schlager, 1998). Accordingly, we concentrate on the interpretation of major disconformities and large-scale depositional cycles that are produced by prominent, high-amplitude fluctuations of relative sea level.

7.1. Time frame

Due to the lack of plankton in the shallow interior platform environment, the biostratigraphic framework is very rough and contains only a few pinning points (Fig. 11). It does, however, yield a latest Rupelian to earliest Chattian age for the studied part of the Shuwayr Formation by the occurrence of *Eulepidina fomosoides* in the basal segment of section MC (beds 3, 4, 7) and *Nephrolepidina* cf. *morgani* in the middle segment of section MC (beds 19, 27, 29, 37, 47). The stratigraphic range of *Eulepidina fomosoides* is late Rupelian to early Chattian (SBZ22a and lower part of SBZ22b of Cahuzac and Poignant, 1997), while *Nephrolepidina* cf. *morgani* has a range from the early Chattian to early Burdigalian (SBZ22b to SBZ25). Both taxa do not occur together in a fossil assemblage. This locates the Rupelian/Chattian boundary between beds MC8 and MC19.

Based on gastropod faunas, an Oligocene (Chattian) age is indicated for the Warak Formation by the occurrence of *Terebra perturrita*, *Conorbis protensus*, *Rhinoclavis submelanoides*, *Gourmya baluchistanensis*, and *Capulus anceps* (Harzhauser, 2007). *Ceritium rude* occur in the Warak Formation as well as in the Ghubbarrah Formation. This gastropod is recorded from the Late Oligocene to the Miocene (Harzhauser, 2007). *Warakia pilleri* and *Cantharidus elkeae* also occur in the Warak Formation as well as in the Gubbarrah Formation. Although both taxa are exclusively known from the studied sections, they have close relatives in the Early Miocene faunas of Indonesia (Harzhauser, 2007). For the Ghubbarrah Formation the occurrence of the gastropods *Pachycrommium harrisi* and *Mitra* cf. *dufresni* indicates an early to middle Miocene age (Harzhauser, 2007). Associated are *Dilatilabrum sublatissimus*, *Campanile pseudoobeliscus*, and *Gourmya delbosi*. These taxa appeared during the Oligocene and persisted into the Aquitanian. Therefore an Aquitanian age is deduced for the Ghubbarrah Formation by Harzhauser (2007).

7.2. Sequence-stratigraphic correlation of major emersion and restriction episodes

The latest Rupelian to earliest Aquitanian time interval includes four major exposure and restriction episodes in the studied sedimentary record, which formed when loss of accommodation was important during important sea level lowstands or a massive sea level fall. These correlate with three sea level lowstands and one late sea level highstand of third-order in the sequence-chronostratigraphic chart of Hardenbol et al. (1998) (Fig. 12). The recognition of the Rupelian/Chattian boundary between beds 7 and 19 in section MC assigns the karstified surface at the base of the oldest large-scale depositional cycle (LI) to the Ru4/Ch1 sequence boundary of Hardenbol et al. (1998). The next emersion event documented by the karst on top of cycle LI then correlates with the Ch2 sequence boundary of Hardenbol et al. (1998). The dolomite cap on top of cycle LII is suggested to correlate with the late highstand before sequence boundary Ch3 of Hardenbol et al. (1998). Unfortunately, the Ch3 sequence boundary is not exposed because of the insufficient outcrop situation on the plain of Madrakah Peninsula (Fig. 2B). A further emergence period is indicated by caliche crusts at the top of LIII. It corresponds with the Chattian/Aquitanian boundary (Harzhauser, 2007) and, therefore, clearly matches the Ch4/Aq1 sequence boundary of Hardenbol et al. (1998).

7.3. Subsidence

The Shuwayr Formation formed during an active phase of extension in the Gulf of Aden that involved continuous subsidence (Fournier et al., 2004). During deposition of the basal argillaceous part of the Shuwayr Formation (Fig. 3), the lack of intertidal and supratidal facies imply that subsidence was relatively strong and created so much accommodation space that subtidal conditions were continuously afforded. The deposition of peritidal carbonate cycles above the Ru4/Ch1 sequence boundary implies that subsidence rate had declined to such a point that the platform was elevated into the intertidal zone during low-amplitude lowstands of relative sea level.

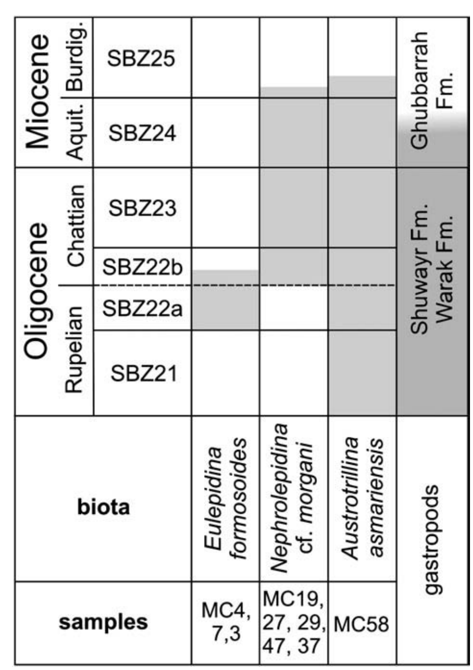

Fig. 11. Biostratigraphy. The distribution of rare biostratigraphic markers in the sampled sections on Madrakah Peninsula and their stratigraphic range indicate latest Rupelian and Chattian age for the Shuwayr and Warak formations, and an Aquitanian age for the Ghubbarrah Formation; SBZ = shallow benthic zone after Cahuzac and Poignant (1997).

Please cite this article as: Reuter, M., et al., Termination of the Arabian shelf sea: Stacked cyclic sedimentary patterns and timing (Oligocene/Miocene, Oman), Sedimentary Geology (2008), doi:10.1016/j.sedgeo.2008.09.001

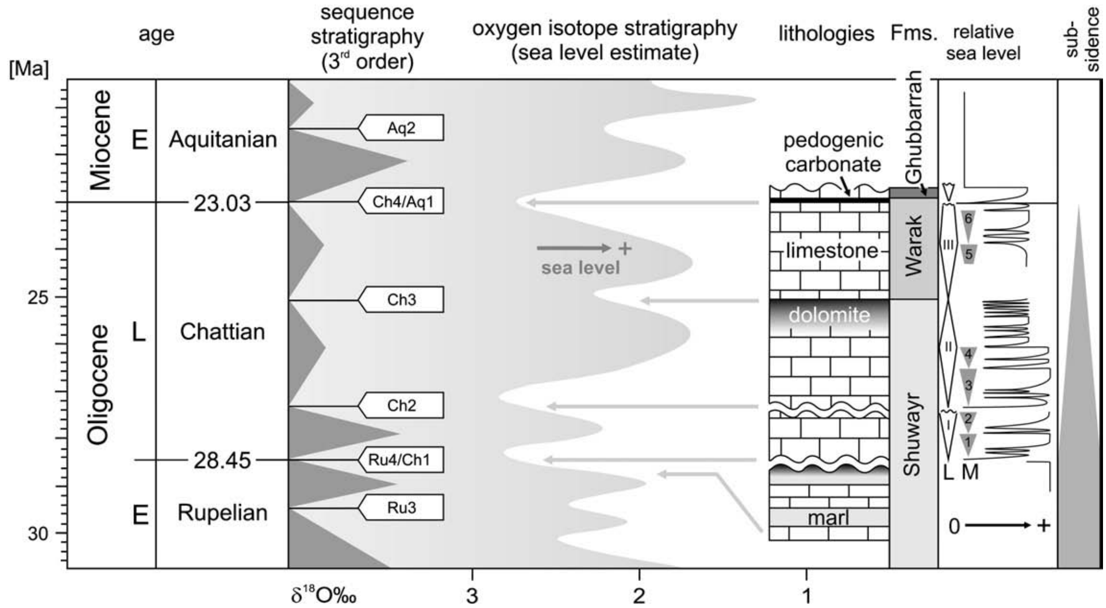

Fig. 12. Stratigraphic correlation of the transitional Oligocene/Miocene succession on Madrakah Peninsula with third-order sequences of Hardenbol et al. (1998) as well as with the isotope curve of Abreu and Haddad (1998). The isotope record roughly reflects sea level. Light grey triangles indicate medium-scale cycles (M) in Figs. 3, 7, 9B, the white triangles represent large-scale depositional cycles (L) in Figs. 3, 7. Chronostratigraphy after Gradstein et al. (2004), lithostratigraphy after Platel et al. (1992a, b) and Béchennec et al. (1993).

This interpretation helps explain the conspicuous lack of cyclicity in older shallow marine carbonate shelf deposits in Oman, although these deposits comprise comparable shallow marine depositional systems and facies-types as described in this study. To date, this has been considered to reflect bio-retexturing by widespread seagrasses and mangroves (Beavington-Penny et al., 2006). However, this interpretation is insufficient because mangrove and seagrass ecosystems are also omnipresent in the cyclic section studied by us.

The Warak Formation does not comprise any open-marine subtidal facies (Figs. 7, 9), which we ascribe to the continuous long-term decrease of accommodation space provided by subsidence during the Late Oligocene. A subsequent marine interval is documented by the Ghubbarrah Formation (Figs. 7, 9) that was formed during the last marine incursion on the Arabian Plate (Platel et al., 1992b). Maximum regression was reached at the Ch4/Aq1 sequence boundary, which is suggested to coincide with the uplift of the rift shoulder at the beginning of the spreading in the Gulf of Aden. The subtidal facies of the overlying Ghubbarrah Formation then testifies to renewed relative sea level rise. However, regardless of the sea level rise, the Jiddat-Arkad Platform emerged permanently soon after, because tectonic uplift overtook the sea level rise.

8. Conclusions

(1) The Shuwayr, Warak and Ghubbarrah formations were deposited on a shallow carbonate platform that was situated on the northeastern rift shoulder of the Gulf of Aden, far away from a hinterland. The sedimentary environments comprised tidal mudflats near mangroves as well as subtidal sandy lagoons with small coral patch reefs, extensive *Acropora* carpets, and seagrass meadows.

(2) During the Late Oligocene, rifting in the Gulf of Aden declined. The end of the rifting was accompanied by a decreasing subsidence and the development of stacked peritidal carbonate cycles. Three hierarchies of depositional cycles are recognised and document a fluctuating relative sea level at different frequencies: (i) small-scale depositional cycles, (ii) medium-scale depositional cycles, and (iii) large-scale depositional cycles.

(3) The depositional model suggests that peritidal cycles could have developed only at the end of the synrift stage when the subsidence rate had declined to the point that the platform was elevated into the peritidal zone where also low amplitudes of high-frequency fluctuations of relative sea level were recorded.

(4) The stratigraphic scheme for the Shuwayr, Warak and Ghubbarrah formations is improved by new biostratigraphic data from benthic foraminifera and gastropods. Based on the biostratigraphic framework, the major exposure events recognised in palaeokarst features and caliche crusts are attributed to the Ru4/Ch1, Ch2, and Ch4/Aq1 third-order sequence boundaries (Hardenbol et al., 1998). Several tens-of-metres-thick early diagenetic dolomitization indicate an important restriction episode and is correlated with the late highstand before the Ch3 sequence boundary.

(5) The reconstructed uplift history of the Jiddat-Arkad Platform shows that the area of southeast Oman was a region along the Tethyan Seaway that became emerged and produced an early, permanent restriction of the marine passage between Africa and Eurasia already during the early Aquitanian.

Acknowledgements

We are indebted to Salim Al Busaidi (Ministry of Commerce and Industry of the Sultanate of Oman) for his kind support and friendly discussions. Jean-Paul Breton (Exploration Consultants, Muscat) and Michaela Bernecker (Erlangen University) provided logistic support. Ortwin Schultz (Natural History Museum Vienna) is thanked for identifying sphyraenid teeth. The article benefits from the helpful reviews of Andre Strasser (University of Fribourg) and Wolfgang Schlager (Vrije University, Amsterdam) and the editorial advises of Chris Fielding (University of Durham). Wolfgang Blendinger (TU Clausthal) reviewed an earlier version of the manuscript. Financial support by the FWF (Project P-18189-N10) is gratefully acknowledged.

References

Abbate, E.P., Balestrieri, M.L., Bigazzi, G., 2001. Uplifted rift-shoulder of the Gulf of Aden in northwestern Somalia: palinspastic reconstructions supported by apatite fission-track data. In: Ziegler, P.A., Cavazza, W., Robertson, A.H.F., Crasquin-Soleau, S. (Eds.), Peri-Tethys Memoir 6: Peri-Tethyan Rift/Wrench Basins and Passive Margins. Mémoirs du Muséum Nationale d'Histoire Naturelle, vol. 186, pp. 629–640.

Abreu, V.S., Haddad, G.A., 1998. Glacioeustatic fluctuations: the mechanism linking stable isotope events and sequence stratigraphy from the early Oligocene to middle Miocene time. In: Graciansky, C.P., Hardenbol, J., Jacquin, T., Vail, P.R. (Eds.),

Mesozoic and Cenozoic Sequence Stratigraphy of European Basins. Society for Sedimentary Geology Special Publication 60, pp. 245–260.
Adams, C.G., Gentry, A.W., Whybrow, P.J., 1983. Dating the terminal Tethyan event. Utrecht Micropaleontological Bulletin 30, 273–298.
Beavington-Penny, S.J., Wright, V.P., Racey, A., 2006. The middle Eocene Seeb Formation of Oman: an investigation of acyclicity, stratigraphic completeness, and accumulation rates in shallow marine carbonate settings. Journal of Sedimentary Research 76, 1137–1161.
Béchennec, F., Le Métour, J., Platel, J.-P., Roger, J., 1993. Geological Map of the Sultanate of Oman. Scale 1:1.000.000, Explanatory Notes. Ministry of Petroleum and Minerals, Sultanate of Oman.
Bernecker, M., 2006. Geologische und paläobiologische Prozesse als Steuerungsfaktoren für die Ausbreitung von scleracinen Korallen am Anfang des Meso- und des Känozoikums. Habil. Thesis, Friedrich-Alexander Universität Erlangen-Nürnberg, pp. 1–223.
Bosselini, A., 1989. Dynamics of Tethyan carbonate platforms. In: Crevello, P.D., Wilson, J.L., Sarg, F., Read, J.F. (Eds.), Controls on Carbonate Platform and Basin Development. Society of Economic Paleontologists and Mineralogists, Special Publication 44, pp. 3–15.
Cahuzac, B., Poignant, A., 1997. Essai de biozonation de l'Oligo-Miocène dans les bassins européens à l'aide des grands foraminifères néritiques. Bulletin Société Géologique de France 168, 155–169.
Camp, V., Robol, M., 1992. Upwelling asthenosphere beneath western Arabia and its regional implications. Journal of Geophysical Research 97, 15,255–15,271.
Cigliano, M., Cocito, S., Gambi, C., 2006. Epibiosis of *Calpensia nobilis* (Esper) (Bryozoa: Cheilostomida) on *Posidonia oceana* (L.) Delile rhizomes: effects on borer colonization and morpho-chronological features of the plant. Aquatic Botany 86, 30–36.
Cowan, C.A., James, N.P., 1992. Diastasis cracks: mechanically generated synaeresis-like cracks in Upper Cambrian shallow water oolite and ribbon carbonates. Sedimentology 39, 1101–1118.
Davis, R.A., Fitzgerald, D.M., 2004. Beaches and Coasts. Blackwell, Oxford, p. 419.
Daradich, A., Mitrovica, J., Pysklywec, R., Willet, S., Forte, A., 2003. Mantle flow, dynamic topography, and rift-flank uplift of Arabia. Geology 31, 901–904.
Demicco, R.V., 1998. CYCOPATH 2-D, a two-dimensional, forward model of cyclic sedimentation on carbonate platforms. Computers and Geosciences 24, 405–423.
Drummond, C.N., Wilkinson, B.H., 1993. Aperiodic accumulation of cyclic peritidal carbonate. Geology 21, 1023–1026.
Filbrandt, J.B., Nolan, S.C., Ries, A.C., 1990. Late Cretaceous and early Tertiary evolution of Jebel Ja'alan and adjacent areas, NE Oman. In: Robertson, A.H.F., Searle, M.P., Ries, A.C. (Eds.), The Geology and Tectonics of the Oman Region. Geological Society of London, Special Publication 49, pp. 697–714.
Flügel, E., 2004. Microfacies of Carbonate Rocks — Analysis, Interpretation and Application. Springer, Berlin-Heidelberg-New York, p. 976.
Fournier, M.N., Bellahsen, O., Gunnell, Y., 2004. Oblique rifting and segmentation of the NE Gulf of Aden passive margin. Geochemistry, Geophysics, Geosystems (G^3) 5. doi:10.1029/2004GC000731.
Gischler, E., 2008. Accretion patterns in Holocene tropical coral reefs: do massive coral reefs in deeper water with slowly growing corals accrete faster than shallower branched coral reefs with rapidly growing corals? International Journal of Earth Sciences 97, 851–860.
Gischler, E., Hudson, J.H., 1998. Holocene development of three isolated carbonate platforms, Belize, Central America. Marine Geology 144, 333–347.
Goldhammer, R.K., Dunn, P.A., Hardie, L.A., 1990. Depositional cycles, composite sea-level changes, cycle stacking patterns, and the hierarchy of stratigraphic forcing; examples from Alpine Triassic platform carbonates. Geological Society of America Bulletin 102, 535–562.
Gradstein, F.M., Ogg, J.G., Smith, A.G., Bleeker, W., Lourens, L.J., 2004. A new geologic time scale with special reference to Precambrian and Neogene. Episodes 27, 83–100.
Haas, J., Lobitzer, H., Monostori, M., 2007. Characteristics of the Lofer cyclicity in the type locality of the Dachstein limestone (Dachstein Plateu, Austria). Facies 53, 113–126.
Hardenbol, J., Thierry, J., Farley, M.B., Jacquin, T., Graciansky, P.-C., Vail, P.R., 1998. Mesozoic and Cenozoic sequence chronostratigraphic framework of European basins. In: Graciansky, C.- P., Hardenbol, J., Jacquin, T., Vail, P.R. (Eds.), Mesozoic and Cenozoic Sequence Stratigraphy of European Basins. Society for Sedimentary Geology, Special Publication 60, pp. 13–603.
Harzhauser, M., 2007. Oligocene and Aquitanian gastropod faunas from the Sultanate of Oman and their biogeographic implications for the early western Indo-Pacific. Palaeontographica 280, 75–121.
Harzhauser, M., Kroh, A., Mandic, O., Piller, W.E., Göhlich, U., Reuter, M., Berning, B., 2007. Biogeographic responses to geodynamics: a key study all around the Oligo-Miocene Tethyan Seaway. Zoologischer Anzeiger — A Journal of comparative Zoology 246, 241–256.
Harzhauser, M., Mandic, O., Piller, W.E., Reuter, M., Kroh, A., 2008. Tracing back the origin of the Indo-Pacific mollusc fauna — basal Tridacninae from the Oligocene and Miocene of the Sultanate of Oman. Palaeontology 51, 199–213.
Houbrick, R.S., 1991. Systematic review and functional morphology of the mangrove snails *Terebralia* and *Telescopium* (Potamididae; Prosobranchia). Malacologia 33, 289–338.
Hofrichter, R., 2002. Das Mittelmeer — Fauna, Flora, Ökologie, Band I: Allgemeiner Teil. Spektrum Akademischer Verlag, Heidelberg, Berlin, p. 607.
Huchon, P., Khanbari, K., 2003. Rotation of the syn-rift stress field of the northern Gulf of Aden margin, Yemen. Tectonophysics 364, 147–166.
Hughes Clarke, M.W., Keij, A.J., 1973. Organisms as producers of carbonate sediment and indicators of environment in the southern Persian Gulf. In: Purser, B.H. (Ed.), The Persian Gulf. Holcene Carbonate Sedimentation and Diagenesis in a Shallow Epicontinental Sea. Springer-Verlag, pp. 33–56.
Hughes, G.W., Varol, O., Beydoun, Z.R., 1991. Evidence for Middle Oligocene rifting of the Gulf of Aden and Late Oligocene rifting of the southern Red Sea. Marine and Petroleum Geology 8, 354–358.
Jones, B., 1992. Void-filling deposits in karst terrains of isolated oceanic islands: a case study from Tertiary carbonates of the Cayman Islands. Sedimentology 39, 857–876.
Jones, R.W., 1999. Marine invertebrate (chiefly foraminiferal) evidence for the palaeogeography of the Oligocene-Miocene of western Eurasia, and consequences for terrestrial vertebrate migration. In: Agusti, J., Rook, L., Andrews, P. (Eds.), Hominid Evolution and Climatic Change in Europe. The Evolution of Neogene Terrestrial Ecosystems in Europe, vol. 1. Cambridge University Press, pp. 274–308.
Jones, R.W., Racey, A., 1994. Cenozoic stratigraphy of the Arabian Peninsula and Gulf. In: Simmons, M.D. (Ed.), Micropalaeontology and Hydrocarbon Exploration in the Middle East. Chapman and Hall, London, pp. 273–307.
Kathiresan, K., Bingham, B.L., 2001. Biology of mangroves and mangrove ecosystems. Advances in Marine Biology 40, 81–251.
Klappa, C.F., 1980. Rhizoliths in terrestrial carbonates: classification, recognition, genesis and significance. Sedimentology 27, 613–629.
Lawrence, J.M., Agatsuma, Y., 2001. The ecology of *Tripneustes*. In: Lawrence, J.M. (Ed.), Edible Sea Urchins: Biology and Ecology. Developments in Aquaculture and Fisheries Science. Elsevier, Amsterdam, pp. 395–413.
Lighty, R.G., Mcintyre, I.G., Stuckenrath, R., 1982. *Acropora palmata* reef framework: a reliable indicator of sea level in the western Atlantic for the past 10,000 years. Coral Reefs 1, 125–130.
Paterson, R.J., Whitaker, F.F., Jones, G.D., Smart, P.L., Waltham, D., Felce, G., 2006. Accommodation and sedimentary architecture of isolated icehouse carbonate platforms: insights from forward modelling with CARB3D$^+$. Journal of Sedimentary Research 76, 1162–1182.
Piller, W.E., Riegl, B., 2003. Vertical versus horizontal growth strategies of coral frameworks (Tulamben, Bali, Indonesia). International Journal of Earth Sciences 92, 511–519.
Platel, J.-P., Roger, J., Peters, T.J., Mercolli, I., Kramers, J.D., Le Métour, J., 1992a. Geological map of Salalah, Sultanate of Oman, sheet NE 40-09, scale 1:250,000, Ministry of Petroleum and Minerals, Muscate, Sultanate of Oman.
Platel, J.-P., Dubreuilh, J., Le Métour, J., Roger, J., Wyns, R., Béchennec, F., Berthiaux, A., 1992b. Geological map of Duqm and Madraca. Sheet NE 40-03/07 Scale 1:250.000, Explanatory Notes, 1–69. Ministry of Petroleum and Minerals, Sultanate of Oman.
Pratt, B.R., James, N.P., Cowan, C.A., 1992. Peritidal carbonates. In: Walker, R.G., James, N.P. (Eds.), Facies Models—Response to Sea Level Change. Geological Association of Canada, Toronto, pp. 303–322.
Renema, W., Troelstra, S.R., 2001. Larger foraminifera distribution on a mesotrophic carbonate shelf in SW Sulawesi (Indonesia). Palaeogeography, Palaeoclimatology, Palaeoecology 175, 125–146.
Rögl, F., 1998. Palaeogeographic considerations for Mediterranean and Paratethys seaways (Oligocene to Miocene). Annalen des Naturhistorischen Museums in Wien 99A, 279–310.
Roger, J., Platel, J.-P., Cavelier, C., Bourdillon-de-Grisac, C., 1989. Données nouvelles sur la stratigraphie et l'histoire géologique du Dhofar (Sultanat d'Oman). Bulletin de la Société Géologique de France 2, 265–277.
Schlager, W., 1998. Exposure, drowning and sequence boundaries on carbonate platforms. In: Camoin, G.F., Davies, P.J. (Eds.), Reefs and Carbonate Platforms in the Pacific and Indian Oceans. International Association of Sedimentologists, Special Publication 25, pp. 3–22.
Schlager, W., 2005. Carbonate sedimentology and sequence stratigraphy. SEPM Concepts in Sedimentology, pp. 1–198.
Sen Gupta, B.K., 1999. Foraminifera in marginal marine environments. In: Sen Gupta, B.K. (Ed.), Modern Foraminifera. Kluwer Academic Publishers, Dordrecht, pp. 141–159.
Soong, K., Chen, T., 2003. Coral transplantation: regeneration and growth of *Acropora* fragments in a nursery. Restoration Ecology 11, 62–71.
Strasser, A., 1991. Lagoonal-p Shark Valley Visitor Centre eritidal sequences in carbonate environments: autocyclic and allocyclic processes. In: Einsele, G., Ricken, W., Seilacher, A. (Eds.), Cycles and Events in Stratigraphy. Springer-Verlag, pp. 709–721.
Strasser, A., Pittet, B., Hillgärtner, H., Pasquier, J.-P., 1999. Depositional sequences in shallow carbonate-dominated sedimentary systems: concepts for a high-resolution analysis. Sedimentary Geology 128, 201–221.
Vargas-Ángel, B., Thomas, J.D., Arke, S.M., 2003. High-latitude *Acropora cervicornis* thickets off Fort Lauderdale, Florida, USA. Coral Reefs 22, 465–473.
Vohra, F.C., 1965. Ecology of intertidal *Zostera* flats of Moreton Bay. Part 2. More detailed studies of a dominant animal, *Pyrazus ebenius* (Bruguière, 1792). PhD thesis, University of Queensland, Brisbane.
Watchorn, F., Nichols, G.J., Bosence, D.W.J., 1998. Rift-related sedimentation and stratigraphy, southern Yemen (Gulf of Aden). In: Purser, B., Bosence, D. (Eds.), Sedimentation and Tectonics in the Rift Basins Red Sea—Gulf of Aden. Chapman and Hall, London, pp. 165–189.
Wilson, M.E.J., Lokier, S.W., 2002. Siliciclastic and volcaniclastic influences on equatorial carbonates: insights from the Neogene of Indonesia. Sedimentology 49, 583–601.

Please cite this article as: Reuter, M., et al., Termination of the Arabian shelf sea: Stacked cyclic sedimentary patterns and timing (Oligocene/Miocene, Oman), Sedimentary Geology (2008), doi:10.1016/j.sedgeo.2008.09.001